Tetrahedron 65 (2009) 628–637

Contents lists available at ScienceDirect

Tetrahedron

journal homepage: www.elsevier.com/locate/tet

Synthesis of 3^2-substituted bacteriochlorophyll-*d* analogs and their self-aggregation in a nonpolar organic solvent

Hitoshi Tamiaki *, Yuki Kotegawa, Shin-ichiro Nitta, Shin-ichi Sasaki †, Keisuke Mizutani

Department of Bioscience and Biotechnology, Faculty of Science and Engineering, Ritsumeikan University, Kusatsu, Shiga 525-8577, Japan

ARTICLE INFO

Article history:
Received 6 October 2008
Received in revised form 6 November 2008
Accepted 6 November 2008
Available online 12 November 2008

Keywords:
Allylation
Chlorosome
Chlorophyll
Trifluoromethylation
Zinc complex

ABSTRACT

Zinc complexes of 3^1-epimerically pure 3^2,3^2,3^2-trifluoro-bacteriopheophorbide-*d* methyl ester were prepared and their self-aggregation was examined in 1% (v/v) dichloromethane and hexane by visible and circular dichroism spectroscopies. Both the synthetic 3^1-trifluoromethylated diastereomers gave amorphous self-aggregates in the nonpolar organic solvent, while the corresponding nonfluorinated compounds possessing the 3^1-methyl group formed well-ordered and large oligomers similar to in vivo aggregates of bacteriochlorophyll-*d* in a chlorosome, a main light-harvesting antenna of green photosynthetic bacteria. The difference is ascribed to steric factor of the 3-CF_3 group, which was supported by optical properties of other synthetic zinc 3^1-hydroxy-13^1-oxo-chlorins possessing trifluoromethyl or secondary/tertiary substituents at the 3^1-position in the nonpolar organic solvent.

1. Introduction

Most porphyrins self-aggregate in some media to form insoluble solids. The procedure is useful for their purification by recrystallization. Naturally occurring chlorophyll self-aggregates similarly to give usually amorphous species with many structural defects, which are less fluorescent due to a concentration quenching.[1] Exceptionally, bacteriochlorophylls(BChls)-*c*, *d*, and *e* (see left top drawing of Fig. 1) self-aggregate in a main light-harvesting antenna system of green photosynthetic bacteria, called a chlorosome, to form well-ordered and large oligomers.[2–9] Thus these self-aggregates have less structural defects in a supramolecule and efficiently provide energy-harvesting and migrating materials. In hydrophobic environments including nonpolar organic solvents and aqueous micelles, natural BChls-*c*/*d*/*e* and their model compounds formed similar self-aggregates.[10–27]

Several research works indicated that the following three moieties in a straight line were necessary for chlorosomal self-aggregation of chlorophyllous pigments: (i) hydroxy group, (ii) central coordinatable metal (Mg, Zn or Cd), and (iii) carbonyl group.[28–36] Zinc methyl bacteriopheophorbide-*d* (**4a**, see right top drawing of Fig. 2) possessing 3^1-OH and 13-C=O on its *y*-axis (the N21–N23 line) was a good model for chlorosomal BChls due to its easy

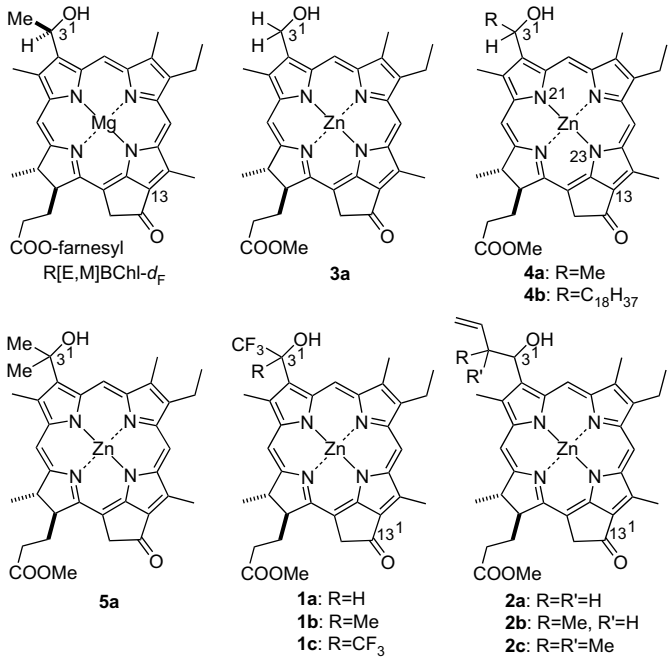

Figure 1. Molecular structures of natural bacteriochlorophyll-*d* (left top) and synthetic zinc methyl bacteriopheophorbides-*d* **1**–**5**.

* Corresponding author. Fax: +81 77 561 2659.
E-mail address: tamiaki@se.ritsumei.ac.jp (H. Tamiaki).
† Present address: Nagahama Institute of Bio-Science and Technology, Nagahama, Shiga 526-0829, Japan.

0040-4020/$ – see front matter © 2008 Elsevier Ltd. All rights reserved.
doi:10.1016/j.tet.2008.11.015

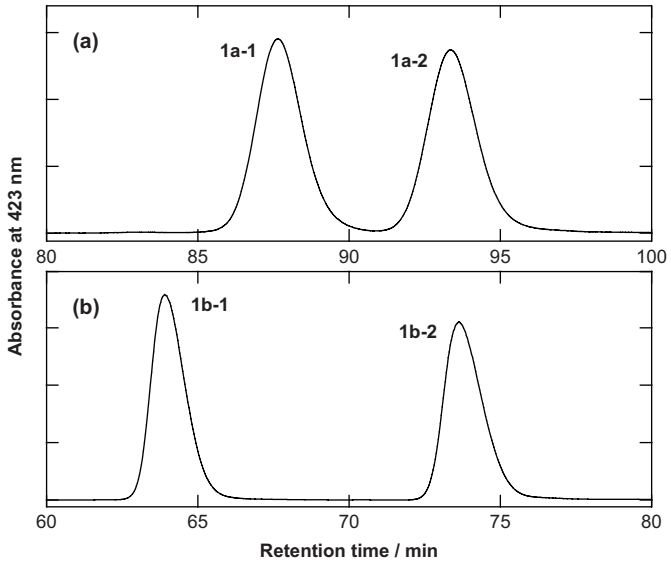

Figure 2. Reverse-phase high performance liquid chromatograms of 3^1-epimeric mixtures of zinc 3-[C*H(CF_3)OH]-chlorin **1a** (a) and zinc 3-[C*CH_3(CF_3)OH]-chlorin **1b** (b); column: Cosmosil $5C_{18}$-ARII $10\varphi\times250$ mm, elution: MeOH/H_2O=8:2, 2.0 ml/min.

availability and high stability.[37–39] Lack of the 3^1-methyl group from **4a** as in **3a** induced tighter self-aggregation[28,40] while addition of a methyl group to the 3^1-position of **4a** as in **5a** did not disturb such self-aggregation.[41] In contrast, substitution of a long alkyl chain (heptadecyl group) at the 3^2-position of **4a** as in **4b** led to formation of some smaller self-aggregates including dimer species, whose supramolecular structures were dependent upon the chirality of 3^1-position.[42]

Here we prepared 3^2,3^2,3^2-trifluorinated derivative **1a** of **4a** and reported self-aggregation of its HPLC-separated 3^1-epimers in 1% (v/v) dichloromethane and hexane. The substitution effect of 3^1-CF_3 group on self-aggregation in the nonpolar organic solvent was investigated by their visible and circular dichroism (CD) spectra. Other zinc 3^1-hydroxy-13^1-oxo-chlorins **1b**/**c** and **2a**–**c** possessing trifluoromethyl or allyl group(s) were synthesized and steric factor of the 3^1-CF_3 was investigated in comparison with their self-aggregation.

2. Results and discussion

2.1. Synthesis of 3^2,3^2,3^2-trifluoro-bacteriochlorophyll-*d* analogs 1a–c

Introduction of a trifluoromethyl group at the 3^1-position in methyl pyropheophorbide was performed by treatment of 3-formyl-chlorin **8a** with trimethyl(trifluoromethyl)silane ($TMSCF_3$) in the presence of tetrabutylammonium fluoride (Scheme 1).[43] After addition of $TMSCF_3$ to the 3-formyl group, the O–Si bond in the resulting adduct was cleaved by action of acid to give desired 3^1-hydroxy-chlorin **6a** (46%). The trifluoromethylation first occurred at the reactive formyl group but undesired trifluoromethylation at the less reactive 13-keto carbonyl group was observed under prolonged reaction conditions. After disappearance of the starting material **8a** by complete shift of the Q_y absorption band from 694 to 667 nm, the reaction had to be quenched immediately by aqueous acidic solution to avoid the above overreaction. The product **6a** gave a new chiral center at the 3^1-position and was found to be a 1:1 epimeric mixture from the ^1H and ^{19}F NMR spectra. No diastereomeric addition was observed under the present achiral reaction conditions because the reactive 3^1-position was far from 17*S*- and 18*S*-chiral centers in a molecule.

The 3-acetyl group in methyl pyropheophorbides was less reactive than the 3-formyl group due to the steric hindrance around the carbonyl group.[44] Trifluoromethylation at the 3^1-position of 3-acetyl-chlorin **8b** was performed less regioselectively. The isolated yield of **6b** decreased to 8%. The product was a 3^1-epimeric mixture (1:1) as expected. The trifluoroacetyl group of **8c** gave a more steric hindrance environment at the 3^1-position than the acetyl group of **8b** (vide infra), but a more electronically positive-charged carbonyl carbon atom.[43] The trifluoromethylation of **8c** thus occurred more regioselectively by substitution of **8b** with three fluoro atoms and the isolated yield of **6c** increased to 29%.

Free bases **6a**–**c** were zinc-metalated to give **1a**–**c** in good yields. The 3^1-epimers of **1a** and **1b** were separated by reverse-phase (RP) HPLC (Fig. 2). The first eluted epimers referred to **1a-1** and **1b-1**, and the second to **1a-2** and **1b-2**. The stereochemistry has not been determined yet, while the first and second eluted epimers of similar zinc complexes (3^1-alkylated secondary alcohols) were reported to be 3^1*R*- and *S*-configurations, respectively.[42] All the synthetic compounds were characterized by their ^1H/^{19}F NMR, visible, and mass spectra.

2.2. Self-aggregation of 1a–c in nonpolar organic solvents

Zinc methyl bacteriopheophorbide-*d* (**4a**) self-aggregated in 1% (v/v) dichloromethane and hexane to give similar large oligomers as chlorosomal aggregates in green photosynthetic bacteria.[41] The self-aggregates of **4a** gave Q_y bands at around 700 nm, which were largely red-shifted from the monomeric band at 648 nm in dichloromethane (Fig. 3a). In 1% CH_2Cl_2/hexane, trifluorinated compound **1a-1** gave shoulders at the red-side of the monomeric Q_y and Soret bands at ca. 670 and 445 nm, respectively (the solid line of Fig. 3b). The deconvolution analysis of the spectrum indicated that broad bands grew by dilution of dichloromethane solution with hexane. The species would be prepared by

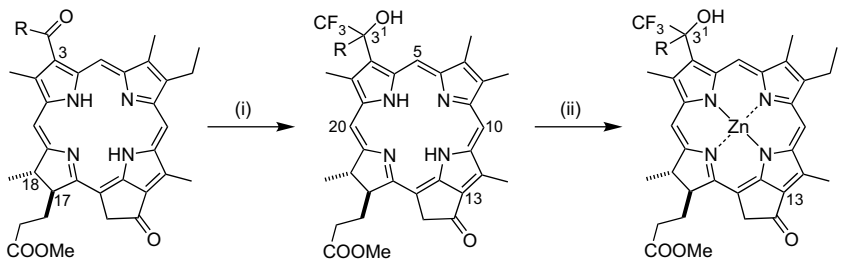

8a: R=H
8b: R=Me
8c: R=CF_3

6a: R=H
6b: R=Me
6c: R=CF_3

1a: R=H
1b: R=Me
1c: R=CF_3

Scheme 1. Synthesis of zinc methyl 3^2,3^2,3^2-trifluoro-bacteriopheophorbides-*d* **1a**–**c**: (i) $TMSCF_3$, $BuN_4F\cdot3H_2O$/THF, and aq HCl; (ii) $Zn(OAc)_2\cdot2H_2O$/MeOH–CH_2Cl_2.

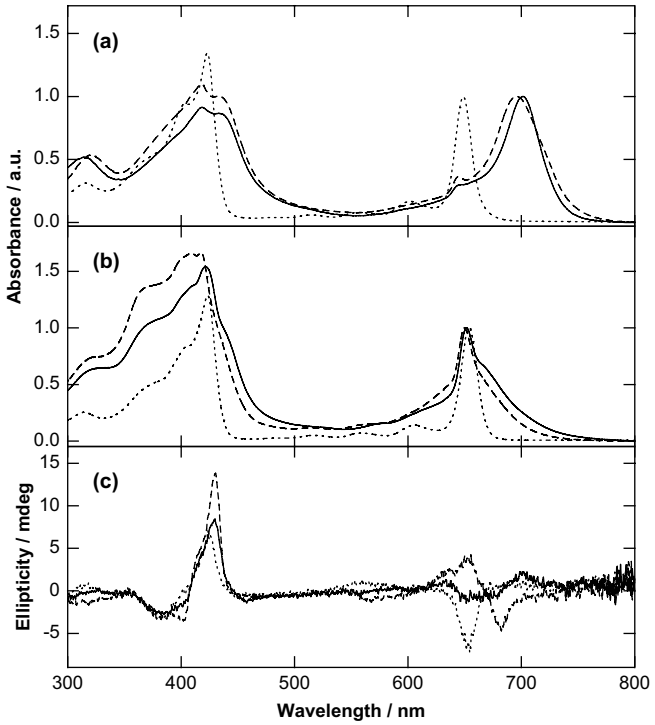

Figure 3. Visible spectra of zinc 3-[C*H(CH_3)OH]-chlorin **4a** (a) and zinc 3-[C*H(CF_3)OH]-chlorin **1a** (b), and CD spectra of **1a** (c); (a) **4aR** (solid line) and **4aS** (broken line) in 1% (v/v) CH_2Cl_2/hexane, and **4aR** (dotted line) in CH_2Cl_2; (b and c) **1a-1** (solid line) and **1a-2** (broken line) in 1% (v/v) CH_2Cl_2/hexane, and **1a-1** (dotted line) in CH_2Cl_2. All the visible spectra were normalized at the Q_y maxima. CD spectra were measured at ca. 10 μM.

coordination of the 3^1-hydroxy group of a molecule with the central zinc of another molecule and various exciton coupling of the molecules afforded the broad bands. The supramolecular structure would be amorphous, while that of $(\mathbf{4a})_n$ was well-ordered.[39,41,45] Therefore, **1a-1** could not give chlorosomal aggregates. Because **1a-1** has 3^1-hydroxy and 13-carbonyl groups as well as central zinc in its *y*-axis requisite for chlorosomal self-aggregation,[13,28,29] the trifluoromethyl group at the 3^1-position disturbed the formation of well-ordered self-aggregates. Small CD bands of **1a-1** in 1% CH_2Cl_2/hexane (solid line of Fig. 3c) supported that the self-aggregate was disordered in a supramolecule.

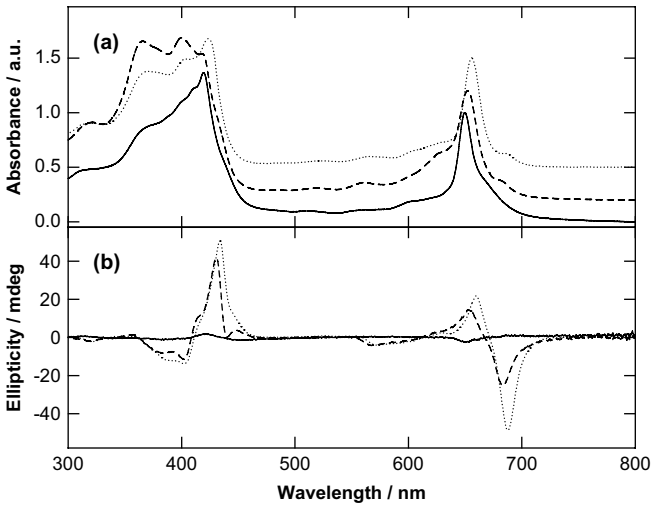

Figure 4. Visible (a) and CD spectra (b) of zinc 3-[CR(CF_3)OH]-chlorins **1b** (R=CH_3) and **1c** (R=CF_3) in 1% (v/v) CH_2Cl_2/hexane; **1b-1** (solid line), **1b-2** (broken line), and **1c** (dotted line). All the visible spectra were normalized at the Q_y maxima. Broken and dotted lines in (a) were drawn in +0.2 and +0.5 addition to the original absorbances, respectively. CD spectra were measured at ca. 10 μM.

Epimeric isomer **1a-2** also gave broad bands as well as monomeric bands in 1% CH_2Cl_2/hexane (broken line of Fig. 3b), and no absorption bands typical of chlorosomal aggregates. The newly appeared bands are pronounced at the blue sides of monomeric bands, compared with those of **1a-1**. The difference was due to the diastereomeric control as seen in **4aR** and **4aS** (Fig. 3a).[39,45] The CD spectrum of **1a-2** in 1% CH_2Cl_2/hexane (broken line of Fig. 3c) showed that a small reverse S-shape band was observed around ca. 670 nm as a zero-crossing point. The bands were similar to that of closed dimer **4bS** prepared by mutual Zn–O coordination and π–π stacking.[42] Such a dimer of **1a-2** would be formed in a small amount. The similarity supported the 3^1-configuration of **1a-2** to be corresponding to that of **4a**/**bS** as well as the elution order did (vide supra). It is noted that such proposed absolute configuration in **1a-2** is termed 3^1R because trifluorination of the 3^1-methyl group in **4aS** changes the sequence of the substituents at the 3^1-position: OH>CF_3>chlorin-3-yl>CH_3>H.

It was reported that zinc methyl 3^1-methyl-bacteriopheophorbide-*d* (**5a**) possessing two methyl groups at the 3^1-position self-aggregated in 1% CH_2Cl_2/hexane to give almost the same oligomer as chlorosomal aggregate of **4aR**.[41] The additional methyl group did not disturb the formation of well-ordered self-aggregates. Addition of a methyl group at the 3^1-position of **1a** as in **1b** induced no formation of chlorosomal aggregates as expected. One epimer **1b-1** in 1% CH_2Cl_2/hexane showed a similar electronic absorption spectrum as **1a-1** (solid lines of Figs. 3b and 4a). The broadened aggregate bands in **1b-1** were relatively smaller than those in **1a-1**. This is ascribable to the steric factor of the additional methyl group. The tertiary alcohol in **1b-1** gave a sterically hindered hydroxy group, which would suppress the formation of the amorphous self-aggregate, while the tertiary OH group in **5a** efficiently produced the well-ordered aggregate. The other epimer **1b-2** in 1% CH_2Cl_2/hexane showed a similar absorption spectrum as **1a-2** (broken lines of Figs. 3b and 4a), where the red-shifted bands decreased and the blue-shifted bands increased. The blue-shifted species might be due to the H-aggregates based on the cofacial dimer with largely π–π stacking and aligning in *y*-axis. The appearance of a large exciton-coupled CD band at Q_y region (broken line of Fig. 4b) indicated that **1b-2** dimerized in a larger amount than **1a-2**. The additional methyl group stabilized such a dimeric species.

Addition of one more trifluoromethyl group to **1a** afforded doubly trifluoromethylated compound **1c**. The absorption spectrum of **1c** in 1% CH_2Cl_2/hexane was similar to that of **1b-2**, and red- and blue-shifted bands were reduced by trifluorination of **1b-2** to **1c**. CD spectra of **1b-2** and **1c** showed that dimeric **1c** was prepared in a slightly larger amount than $(\mathbf{1b\text{-}2})_2$. The trifluoromethyl group at the 3^1-position induced more stabilization of dimeric species than the methyl group, which would be ascribable to the steric factor. A sterically larger CF_3 group suppressed the dissociation of dimeric species.

2.3. Steric factor of 3^1-trifluoromethyl group in self-aggregation of 1a–c

The association constant of zinc methyl pyropheophorbide-*a* (Chart 1) with 1-phenyl-2,2,2-tifluoroethanol in benzene was determined by titration method in visible spectral analysis[46] to be 65 M^{-1} and was about half of that with 1-phenylethanol (120 M^{-1}), indicating that the coordination power of the 3^1-OH in **1a** was comparable to that in **4a**. Steric factor of the 3^1-CF_3 group in **1a** inhibited the formation of chlorosomal aggregates. A fluorine atom has been used to mimic a hydrogen atom due to their close sizes,

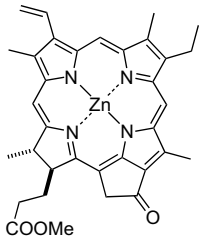

Chart 1.

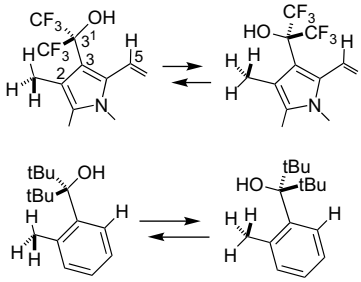

Figure 6. Partial stereodrawings of energy-minimized molecule **1c** by MM+/PM3 calculation (upper) and isolated rotamers of di(*tert*-butyl)-*o*-tolyl-carbinol (lower).

but a trifluoromethyl group is proposed to be larger in size than a methyl group and comparable to an isopropyl group.[47–49]

The 3^1-OH of a molecule coordinated with the central Zn of another molecule, and the coordinated OH hydrogen-bonded with 13-C=O of the third molecule. The special bonding and successive stacking of chlorin π-systems made chlorosomal aggregates.[13,28,29] In trifluoromethylated **1a**, the 3^1-OH coordinated with the Zn as mentioned above, but the coordinated OH could not hydrogen-bond with 13-C=O due to the steric hindrance. Thus, chlorosomal aggregates of **1a** could not be formed in 1% CH_2Cl_2/hexane.

The steric factor of CF_3 groups was investigated in the following NMR study. In 1% (v/v) pyridine-d_5 and $CDCl_3$, **1c** possessing 3-$C(CF_3)_2OH$ gave two sets of ^1H and ^{19}F signals and the ratios were about 1:3 at room temperature. Doubly trifluoromethylated **6c** also afforded 1:2 mixed ^1H and ^{19}F signals in $CDCl_3$. The peaks (2:3) in $CDCl_2CDCl_2$ coalesced at a higher temperature as shown in Figure 5. The results indicated that the separated peaks were due to the atropisomers by rotation around the $3–3^1$ bond. Two sterically large CF_3 groups interfered with the rotation through the interaction of a neighboring 2-methyl group and 5-hydrogen atom to give two rotamers in a solution (Fig. 6). Temperature dependent spectra of **6c** estimated the barrier between the two rotamers to be 17 kcal mol^{-1}.[50] The value was in agreement with the calculated value (18 kcal mol^{-1}) from molecular models based on MM+/PM3 methods (Fig. S1).[51] In **1a**/**b**, **4a**/**b**, **5a**, and **6a**/**b**, no rotamers were observed in their NMR spectra and two CF_3 groups at the 3^1-position were necessary for detection of rotamers in a solution at room temperature.[52] Such rotamers could not be isolated by standard procedures including HPLC at room temperature due to the moderately rotational barrier: usually >23 kcal mol^{-1} as the barrier is requisite to isolate isomers.[54] Di(*tert*-butyl)-*o*-tolyl-carbinol gave two stable rotamers at room temperature where the barrier was 28 kcal mol^{-1} (Fig. 6).[53] Therefore, a CF_3 group was sterically less hindered than a $C(CH_3)_3$ group.

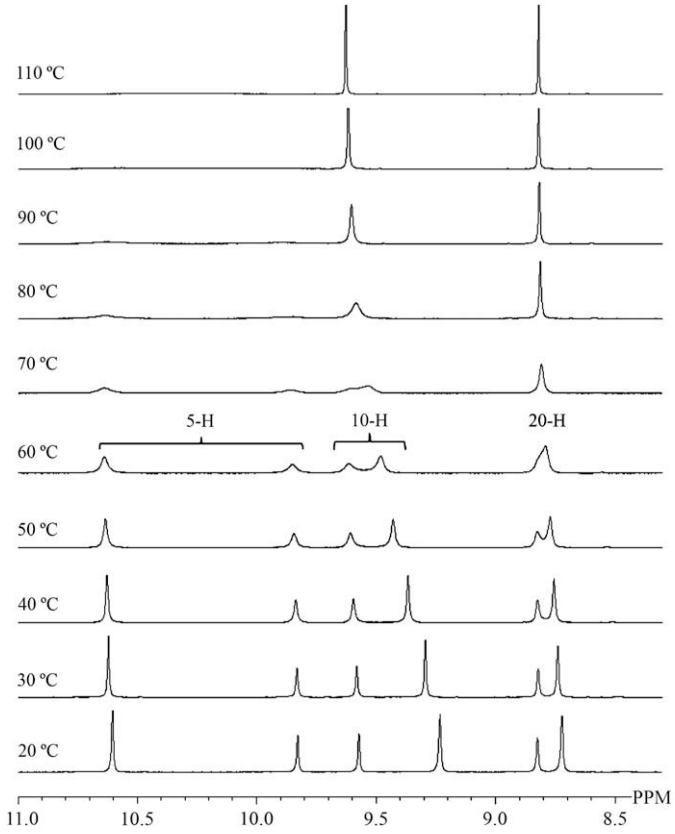

Figure 5. *meso*-Proton signals (600 MHz) of **6c** in $CDCl_2CDCl_2$ at a 10 °C interval from 20 (bottom) to 110 °C (top). The 5-H peaks gave no clear coalescence, which would be ascribed to their larger split.

2.4. Synthesis of 3^2-vinyl-bacteriochlorophyll-*d* analogs 2a–c

The size of a trifluoromethyl group is estimated to be larger than that of a methyl group, comparable to (or larger than) that of an isopropyl group and smaller than that of a *tert*-butyl group (vide supra). To confirm the steric effect of the trifluoromethyl group at 3^1-position in $3^2,3^2,3^2$-trifluorinated **1** on their self-aggregation, we tried to prepare 3^2-methyl-, $3^2,3^2$-dimethyl-, and $3^2,3^2,3^2$-trimethyl-bacteriopheophorbides-*d* **9b–d** (Scheme 2). We have already reported that the 3-formyl group of methyl pyropheophorbide-*d* (**8a**) was methylated by Grignard reaction to give methyl bacteriopheophorbide-*d* (**9a**) in a yield of 75%.[55] Similar treatment of **8a** with ethyl magnesium iodide gave 3^1-ethylated **9b** (75%). In contrast, Grignard reaction of **8a** with isopropyl magnesium chloride gave a complex product, of which successive HPLC purification afforded 3^1-isopropylated **9c** in low yield (<10%). Moreover, 3^1-*tert*-butylated **9d** could not be isolated from the reaction mixture of **8a** with *tert*-butyl magnesium chloride. Under the reaction conditions, primary alkyl groups were successfully introduced at the 3^1-position, but secondary and tertiary alkyl groups were added to the 3-formyl carbon atom in much less and no more quantity, respectively.

To attach secondary and tertiary substituents at the 3^1-position efficiently, Barbier-type allylation was applied.[56] Treatment of **8a** with allyl bromide in the presence of indium powder in an equal volume mixture of aqueous tetrahydrofuran (THF) at room temperature induced quick consumption of **8a** (within 30 min) to give 3^1-allylated **7a** in a 28% yield (Scheme 2).[57] A decrease of the water content suppressed the reaction rate but increased the yield. In H_2O/THF (1:2), the yield of **7a** was optimized to be 80% after stirring for 2 h. Lower addition of water (1:5) required a 20-h reaction for **8a** to disappear and decreased the yield to 15%, and no addition of

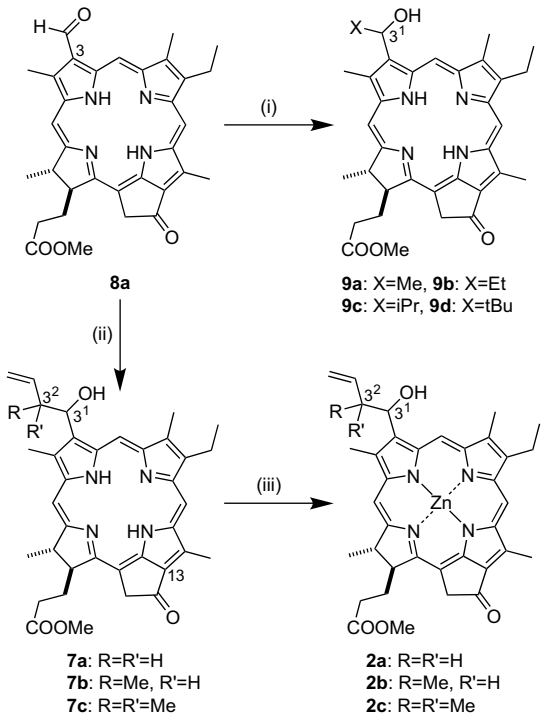

Scheme 2. Synthesis of 3^1-substituted bacteriopheophorbides-*d* **9a–d** and zinc methyl 3^2-vinyl-bacteriopheophorbides-*d* **2a–c**: (i) MeMgI, EtMgI, ^{i}PrMgCl or ^{t}BuMgCl/THF, 0 °C, and aq NH_4Cl; (ii) RR′C=$CHCH_2Br$, In powder/H_2O–THF (1:2) or DMF/NaI; (iii) $Zn(OAc)_2\cdot 2H_2O$/MeOH–CH_2Cl_2.

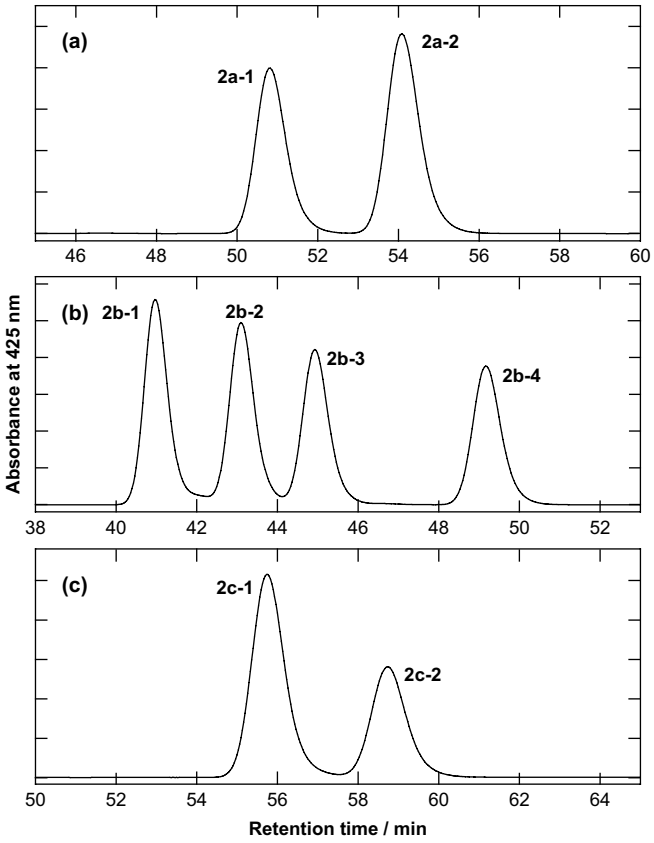

Figure 7. Reverse-phase high performance liquid chromatograms of 3^1,3^2-epimeric mixtures of zinc 3-[C*H(OH)CH_2CH=CH_2]-chlorin **2a** (a), zinc 3-[C*H(OH)C*H-(Me)CH=CH_2]-chlorin **2b** (b), and zinc 3-[C*H(OH)CMe_2CH=CH_2]-chlorin **2c** (c); column: Cosmosil $5C_{18}$-ARII $10\varphi\times250$ mm, elution: MeOH/H_2O=9:1, 1.0 ml/min. All the compounds were prepared via Barbier reactions in an aqueous THF solution.

water as the co-solvent induced no reaction. Under the optimized conditions, the reaction was highly regioselective and no adduct to the 13-keto carbonyl group was observed in the reaction mixture. The ^{1}H NMR spectrum of product **7a** proved it to be a 3^1-epimeric mixture (1:1) and no diastereomeric control was performed under the present reaction conditions.

Indium-promoted Barbier reaction of **8a** with crotyl bromide gave exclusively γ-adduct **7b** (64%) possessing a secondary substituent at the 3^1-position. The reaction proceeded smoothly in spite of the formation of sterically hindered adduct **7b**[58] and the entire amount of **8a** was consumed within 2 h. Similar reaction of **8a** with prenyl bromide gave solely **7c** (42%) possessing a tertiary substituent at the 3^1-position as an isolated adduct. The yields of adducts decreased in the order of **7a**→**7b**→**7c**. Under the above reaction conditions, an increase in the steric hindrance at the reactive γ-site of bromides decreased the yields of **7**: primary>secondary>tertiary. To enhance the reactivity, aqueous THF was changed to *N*,*N*-dimethylformamide (DMF) containing NaI as reported.[59] In dry DMF in the presence of NaI, the yields of **7b** and **7c** were improved to 74 and 61%. In the system, no α-adduct was detected and γ-selectivity was attained predominantly. The products **7b** and **7c** were $3^1/3^2$- and 3^1-epimeric mixtures, respectively. While **7c** was a simple 1:1 mixture as expected, **7b** was a complex mixture of four stereoisomers due to the two adjacent asymmetric centers in the 3-substituent, which is discussed below.

Stereoisomeric mixtures of **7a–c** were zinc-metalated to give **2a–c** efficiently. All the stereoisomers **2a–c** were readily separated by a single run of isocratic RP-HPLC (MeOH/H_2O=9:1). The stereochemically pure compounds were termed as shown in Figure 7: **2a-1** as the first eluted band and **2a-2** as the second, **2b-1**/**2b-2**/**2b-3**/**2b-4** as the first/second/third/fourth, and **2c-1** (first)/**2c-2** (second). The stereochemistry of **2a-1** and **2a-2** was determined to be 3^1R- and 3^1S-configurations, respectively, by modified Mosher's method reported previously:[42] the secondary alcohols were esterified with (*R*)- and (*S*)-α-methoxy-α-(trifluoromethyl)phenylacetyl chloride (MTPA-Cl) and chemical shifts of the resulting MTPA-ester diastereomers were compared (see Fig. S2). The stereochemical determination was consistent with the proposal from the HPLC elution order (vide supra). Since the hydroxy groups of **2b** possessing a secondary substituent at the 3^1-position and **2c** possessing a 3^1-tertiary substituent were less reactive with MTPA-Cl, the configuration at these more sterically hindered 3^1-positions could not be determined by modified Mosher's method. Compared with **2a-1**(=**2aR**) and **2a-2**(=**2aS**), **2c-1** and **2c-2** were tentatively assigned to 3^1R- and 3^1S-epimers.[60]

In the case of **2b**, the stereochemistry was more complicated due to the additional and adjacent 3^2-chiral center. The HPLC profile of **2b** prepared in aqueous THF (Fig. 7b) showed four bands as expected from 3^1- and 3^2-diastereomers. A set of the first two eluted bands (ca. 1:1) was slightly larger than the latter two with 1:1 areas. These two sets were assigned to homochiral *R*–*R*/*S*–*S* and heterochiral *R*–*S*/*S*–*R* diastereomers at the 3^1–3^2 positions. The HPLC analysis of **2b** prepared in DMF/NaI (Fig. S3) showed that the 1:1 set eluted fast was three times larger than the second set. Therefore, **7b** giving the fast moving diastereomers of **2b** were preferentially prepared in the Barbier reaction. MM+/PM3 calculation of four diastereomers **7b** indicated that the heterochiral set were more stable than the homochiral: total energies of $3^1R,3^2R$-, $3^1S,3^2S$-, $3^1R,3^2S$-, and $3^1S,3^2R$-**7b**=72.7, 72.7, 71.8, and 71.8 kcal mol^{-1}. Based on the observed elution pattern and estimated molecular models, **2b-1**/**2b-2** and **2b-3**/**2b-4** were tentatively assigned as heterochiral and homochiral diastereomers, respectively.

2.5. Self-aggregation of 2a–c in nonpolar organic solvents

Mono-vinylation at the 3^2-position of **4aR**/**S** gave **2aR**/**S**, and similar absorption spectra in 1% CH_2Cl_2/hexane were obtained in **2aR** and **4aR** (solid lines of Figs. 8a and 3a) as well as in **2aS** and **4aS** (broken lines of Figs. 8a and 3a). Both the 3^1R-epimers gave more red-shifted Q_y maxima of oligomers, sharper Q_y band of self-aggregates, and less residual Q_y monomers at 645 nm than the corresponding 3^1S-epimers. In the red-shifted regions, large CD bands were observed for **2aR** and **2aS** (Fig. 9a). 3^1-Allylated **2aR**/**S** thus self-aggregated in the nonpolar organic solvents to give chlorosomal oligomers.

Mono-methylation at the 3^2-position of **2aR**/**S** gave **2b-1**, **2b-2**, **2b-3**, and **2b-4** whose absorption spectra in 1% CH_2Cl_2/hexane were dependent on the stereochemistry at the 3^1- and 3^2-positions (Fig. 8b and c). One of the heterochiral isomers **2b-1** showed a similar absorption spectrum as **2aS** (solid line of Fig. 8b and broken line of Fig. 8a) and gave chlorosomal self-aggregates instead of an additional 3^2-methyl group. The other heterochiral isomer **2b-2** had difficulty to self-aggregate, based on the visible spectral analysis shown in Figure 8b. The visible and CD spectra of **2b-2** (broken lines of Figs. 8b and 9b) were similar to those of **1a-2** (broken lines of Fig. 3b and c), indicating that the secondary substituent at the 3^1-position of **2b-2** sterically behaved as the 3^1-trifluoromethyl group in **1a-2**. The above reverse observation in self-aggregation that neither **1a** nor **2b-2** formed the supramolecules of chlorosomal aggregates but that **2b-1** could was explained as follows. A trifluoromethyl group is an isotropic, spherical, and bulky substituent, and the secondary substituents including an isopropyl group are anisotropic.[61] The C–H part of the secondary substituents is less sterically hindered and is able to accommodate any other moieties close by. As a result, **2b-1** possessing the 3^2-H self-aggregated to form a chlorosomal oligomer while neither **2b-2** possessing the stereochemically different 3^2-H nor **1a-1**/**1a-2** possessing 3^1-CF_3 could make chlorosomal aggregates.

3^2-Methyl-3^2-vinyl-compound **2b-3** showed a similar visible spectra as 3^1,3^2-dimethyl-3^2-vinyl-compound **2c-1** in 1% CH_2Cl_2/hexane (solid lines of Fig. 8c and d). They had two Q_y bands at 645 and 654/655 nm, the former ascribed to a residual monomer and the latter to a dimeric species. The similarity in visible spectra was supported by the observation that the two CD spectra were almost the same (solid lines of Fig. 9c and d). Similarities in visible and CD spectra between **2b-4** and **2c-2** were also observed (broken lines of Figs. 8c and d/9c and d). Small changes by additional 3^2-methylation as in **2b-3**/**2b-4**→**2c-1**/**2c-2** indicated the steric factors around the 3^1-hydroxy group important for intermolecular interaction in nonpolar organic solvents were not affected by the methylation. Neither **2b-3**/**2b-4** possessing a 3^1-secondary substituent nor **2c-1**/**2c-2** possessing a 3^1-tertiary substituent could form chlorosomal aggregates but could form sole dimers. Comparing the optical properties of **1a-1**/**1a-2** with those of **2c-1**/**2c-2**, the 3^1-trifluoromethyl group was less sterically hindered than the 3^1-tertiary substituent, $-CMe_2CH{=}CH_2$.

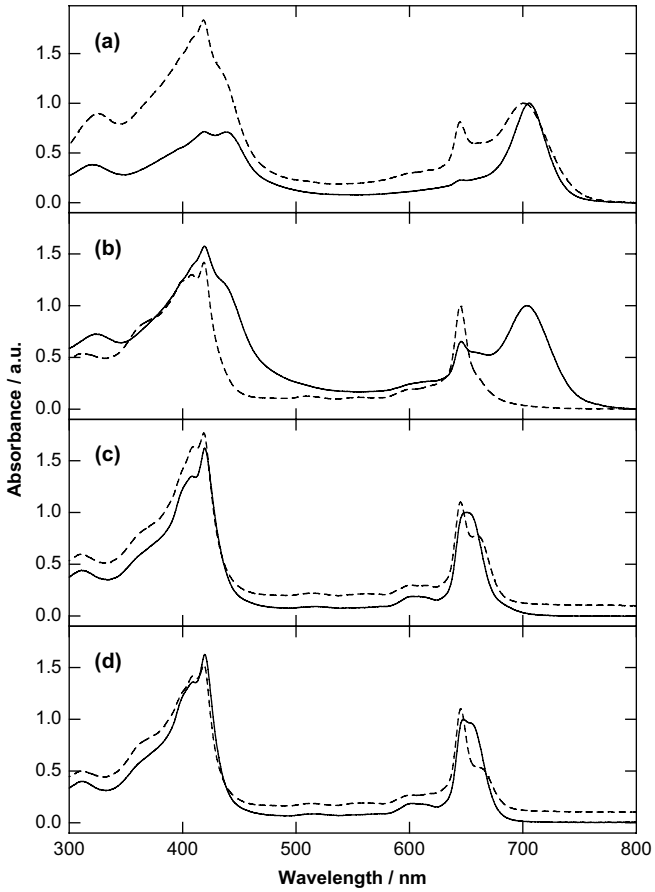

Figure 8. Visible spectra of zinc 3-[C*H(CRR′CH=CH_2)OH]-chlorin **2** in 1% (v/v) CH_2Cl_2/hexane; (a) **2aR** (solid line) and **2aS** (broken line) [R=R′=H]; (b) **2b-1** (solid line) and **2b-2** (broken line) [R=Me, R′=H]; (c) **2b-3** (solid line) and **2b-4** (broken line) [R=Me, R′=H]; (d) **2c-1** (solid line) and **2c-2** (broken line) [R=R′=Me]. All the visible spectra were normalized at the most intense Q_y maxima. Broken lines in (c) and (d) were drawn in +0.2 addition to the original absorbances.

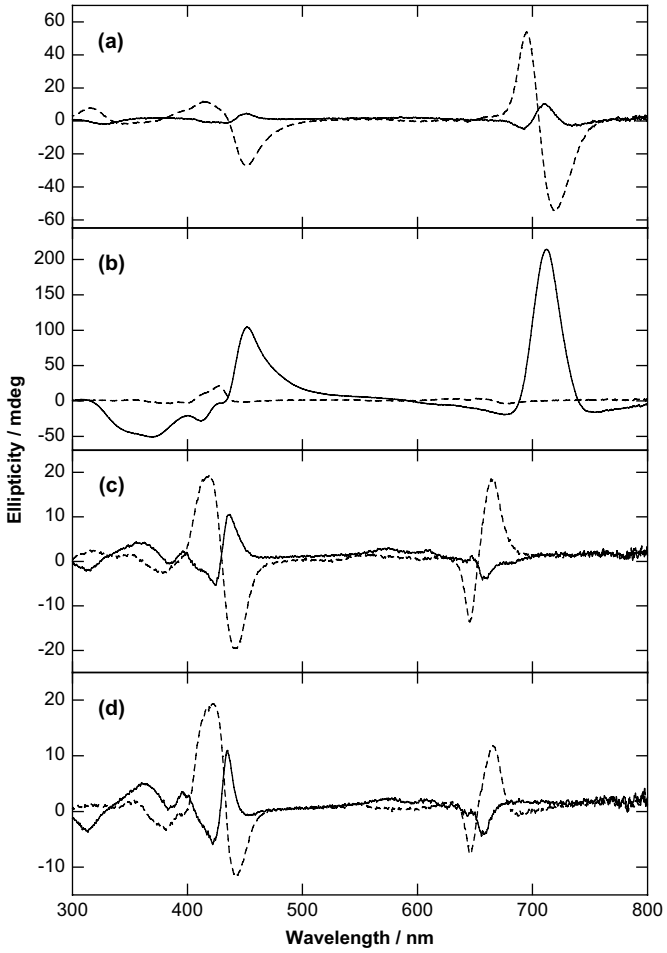

Figure 9. CD spectra of zinc 3-[C*H(CRR′CH=CH_2)OH]-chlorin **2** (ca. 10 μM) in 1% (v/v) CH_2Cl_2/hexane; (a) **2aR** (solid line) and **2aS** (broken line) [R=R′=H]; (b) **2b-1** (solid line) and **2b-2** (broken line) [R=Me, R′=H]; (c) **2b-3** (solid line) and **2b-4** (broken line) [R=Me, R′=H]; (d) **2c-1** (solid line) and **2c-2** (broken line) [R=R′=Me].

Table 1
Q_y absorption data of zinc methyl 3^2-substituted bacteriopheophorbides-*d* possessing 3-[C*H(OH)R]. Redmost Q_y maxima λ_{max} (nm) of their monomers in CH_2Cl_2 and their self-aggregates in 1% (v/v) CH_2Cl_2 and hexane, and red shifts Δ (cm^{-1}) of λ_{max} by self-aggregation

Compound (R, stereochemistry)	λ_{max}		Δ[b]
	Monomer	Self-aggregates[a]	
4aR (Me, 3^1R)	648	702 [900]	1200
4aS (Me, 3^1S)	648	696 [1100]	1050
1a-1 (CF_3, 3^1S[c])	654	665 [≈1400][d]	250
1a-2 (CF_3, 3^1R[c])	653	658 [≈1300][d]	100
2aR ($CH_2CH{=}CH_2$, 3^1R)	651	706 [750]	1200
2aS ($CH_2CH{=}CH_2$, 3^1S)	651	701 [≈1000]	1100
2b-1 (C*HMeCH=CH_2, 3^1R,3^1S[c])	651	704 [≈950]	1150
2b-2 (C*HMeCH=CH_2, 3^1S,3^1R[c])	651	650 [≈900][d]	≈0
2b-3 (C*HMeCH=CH_2, 3^1R,3^1R[c])	651	654 [600][d]	100
2b-4 (C*HMeCH=CH_2, 3^1S,3^1S[c])	651	661 [600][d]	250
2c-1 ($CMe_2CH{=}CH_2$, 3^1R[c])	651	655 [600][d]	100
2c-2 ($CMe_2CH{=}CH_2$, 3^1S[c])	651	662 [600][d]	250

[a] The values in brackets indicate observed full widths at half maxima or estimated band widths (cm^{-1}).
[b] $\Delta=\{1/\lambda_{max}(\text{monomer})-1/\lambda_{max}(\text{aggregates})\}\times10^7$.
[c] Tentative assignment.
[d] Estimated values from curve-fitting analyses.

3. Conclusion

Zinc methyl 3^2-substituted bacteriopheophorbides-*d* possessing 3-[C*H(OH)R] were prepared by modifying methyl pyropheophorbide-*d* possessing the 3-formyl group. These synthetic zinc complexes had both 3^1-hydroxy and 13-keto-carbonyl groups as did BChl-*d*, and self-aggregated in nonpolar organic solvents. The supramolecular structures of the resulting self-aggregates were dependent upon both the 3^1-stereoconfiguration and 3^1-substituents. The data of Q_y bands are summarized in Table 1. Zinc 3^1-hydroxy-13^1-oxo-chlorins possessing a primary substituent at the 3^1-position formed large and well-ordered self-aggregates similar to $(\text{BChl-}d)_n$ in a natural chlorosome. In contrast, zinc chlorins possessing a secondary or tertiary substituent at the 3^1-position as well as 3-CF_3 formed small oligomers including dimers and amorphous self-aggregates except **2b-1**. The difference in self-aggregation was dependent upon the steric factor of the 3^1-substituents. The sterically bulky groups at the 3^1-position suppressed the interactive activity (including hydrogen bonding) of the 3^1-hydroxy group coordinating with the zinc of the other molecule and disturbed the formation of chlorosomal self-aggregates.

4. Experimental

4.1. General

Visible absorption and CD spectra were measured in air-saturated solvents at room temperature on a Hitachi U-3500 spectrophotometer and a Jasco J-720 W spectropolarimeter, respectively. ^1H and ^{19}F NMR spectra were recorded at 293 K on a JEOL ECA-600 (600 and 565 MHz) spectrometer; $CHCl_3$ (δ_H=7.26 ppm) was used as an internal reference and CF_3COOH (δ_F=−77.00 ppm) was used as an external reference. Atmospheric pressure chemical ionization (APCI) and fast atom bombardment-mass spectroscopy (FABMS) data were measured by Shimadzu LCMS-2010EV and JEOL GCmate II spectrophotometers, respectively; methanol solutions were injected for APCIMS and *m*-nitrobenzyl alcohol or glycerol was used as a FABMS matrix. Flash column chromatography (FCC) was performed with silica gel (Merck, Kieselgel 60). HPLC was done with a packed column (Nacalai, Cosmosil 5C_{18}-ARII 10$\varphi\times$250 mm), Shimadzu LC-10ADvp pump, and SPD-M10Avp photodiode array detector.

Methyl $3^2,3^2,3^2$-trifluorobacteriopheophorbide-*d* (**6a**),[43] methyl pyropheophorbide-*d* (**8a**),[28] methyl 3-acetyl-3-devinyl-pyropheophorbide-*a* (**8b**),[62] and methyl 3-devinyl-3-trifluoroacetyl-pyropheophorbide-*a* (**8c**)[43] were prepared according to reported procedures.

4.2. Synthesis of (zinc) methyl 3^1-trifluoromethyl-bacteriopheophorbides-*d*

*4.2.1. Zinc methyl $3^2,3^2,3^2$-trifluorobacteriopheophorbide-d (**1a**)*

Methyl $3^2,3^2,3^2$-trifluorobacteriopheophorbide-*d* (**6a**, $3^1R/S$=1:1, 10 mg) was dissolved in CH_2Cl_2 to which was added a MeOH solution saturated with $Zn(OAc)\cdot2H_2O$ and the mixture was stirred for 2 h at room temperature. Completion of the reaction was confirmed by the absorption spectral change (Q_y peak maximum, 667→654 nm). The reaction mixture was washed with aqueous 4% $NaHCO_3$ and water, dried over Na_2SO_4, and evaporated to dryness. The crude product was purified by FCC (MeOH/CH_2Cl_2=3:97) to give **1a** (8 mg, 80%) as a green solid. The 3^1-epimeric mixture (1:1) was separated by HPLC (MeOH/H_2O=8:2, 2.0 ml/min) to afford the first eluted **1a-1** and the second **1a-2** at retention time=88 and 93 min, respectively. Compound **1a-1**: UV–vis (CH_2Cl_2) λ_{max}=654 (rel intensity, 0.78), 606 (0.11), 558 (0.05), 516 (0.03), 423 nm (1.00); ^1H NMR ($CDCl_3$/1%C_5D_5N) δ=9.60, 9.56, 8.37 (each 1H, s, 5-, 10-, 20-H), 6.55 (1H, q, J=7 Hz, 3-CH), 5.18, 5.07 (each 1H, d, J=20 Hz, 13^1-CH_2), 4.38 (1H, q, J=8 Hz, 18-H), 4.19 (1H, dt, J=8, 2 Hz, 17-H), 3.72 (2H, q, J=8 Hz, 8-CH_2), 3.68, 3.55, 3.41, 3.22 (each 3H, s, 2-, 7-, 12-CH_3, $COOCH_3$), 2.58–2.51, 2.40–2.32, 2.28–2.20, 1.97–1.90 (each 1H, m, 17-CH_2CH_2), 1.70 (3H, d, J=8 Hz, 18-CH_3), 1.68 (3H, t, J=8 Hz, 8^1-CH_3); ^{19}F NMR ($CDCl_3$/1%C_5D_5N) δ=−77.37 (3F, d, J=6 Hz, 3^1-CF_3); MS (APCI) found: m/z 683.3, calcd for $C_{34}H_{34}F_3N_4O_4Zn$: MH^+, 683.2. Compound **1a-2**: UV–vis (CH_2Cl_2) λ_{max}=653 (rel, 0.73), 606 (0.11), 558 (0.06), 516 (0.04), 423 nm (1.00); ^1H NMR ($CDCl_3$/1%C_5D_5N) δ=9.63, 9.56, 8.36 (each 1H, s, 5-, 10-, 20-H), 6.54 (1H, q, J=7 Hz, 3-CH), 5.18, 5.07 (each 1H, d, J=20 Hz, 13^1-CH_2), 4.38 (1H, q, J=8 Hz, 18-H), 4.19 (1H, dt, J=8, 2 Hz, 17-H), 3.72 (2H, q, J=8 Hz, 8-CH_2), 3.68, 3.55, 3.39, 3.22 (each 3H, s, 2-, 7-, 12-CH_3, $COOCH_3$), 2.58–2.51, 2.40–2.32, 2.28–2.20, 1.97–1.90 (each 1H, m, 17-CH_2CH_2), 1.68_2 (3H, d, J=8 Hz, 18-CH_3), 1.67_6 (3H, t, J=8 Hz, 8^1-CH_3); ^{19}F NMR ($CDCl_3$/1%C_5D_5N) δ=−77.46 (3F, d, J=6 Hz, 3^1-CF_3); MS (APCI) found: m/z 683.3, calcd for $C_{34}H_{34}F_3N_4O_4Zn$: MH^+, 683.2.

*4.2.2. Methyl 3^1-trifluoromethyl-bacteriopheophorbide-d (**6b**)*

To a solution of methyl 3-acetyl-3-devinyl-pyropheophorbide-*a* (**8b**, 26 mg, 0.041 mmol) in THF (5 ml) was added $TMSCF_3$ (48 mg, 0.34 mmol) and $Bu_4NF\cdot3H_2O$ (5 mg, 0.016 mmol), and the mixture was stirred for 5 min at room temperature. Completion of the reaction was confirmed by the absorption spectral change (Q_y peak maximum, 682→668 nm). An aqueous 10% HCl solution (2 ml) was added and the reaction mixture was further stirred for 1 h. The mixture was poured into H_2O and extracted with CH_2Cl_2. The extract was washed successively with H_2O and brine, dried over anhydrous Na_2SO_4, filtered, and concentrated. The crude product was purified by FCC (Et_2O/CH_2Cl_2=8:92) to give **6b** (2 mg, 8%) as a $3^1R/S$ mixture (1:1): black solid. UV–vis (CH_2Cl_2) λ_{max}=668 (rel, 0.53), 611 (0.07), 540 (0.10), 508 (0.09), 410 nm (1.00); ^1H NMR ($CDCl_3$) δ=10.34/28, 9.52/46, 8.69/64 (each 1H, s, 5-, 10-, 20-H), 5.25/11, 5.12/04 (each 1H, d, J=19 Hz, 13^1-CH_2), 4.50 (1H, dq, J=2, 7 Hz, 18-H), 4.30/22 (1H, d, J=9 Hz, 17-H), 3.71 (2H, m, 8^1-CH_2), 3.65/64, 3.62/60, 3.57/55, 3.27/26, (each 3H, s, 2-, 7-, 12-CH_3, $COOCH_3$), 2.63 (3H, s, 3^1-CH_3), 2.70–2.53, 2.33–2.19 (each 2H, m, 17-CH_2CH_2), 1.82/81 (3H, d, J=8 Hz, 18-CH_3), 1.70/69 (3H, t, J=8 Hz, 8-CH_3), 0.05/−0.12, −1.97/

−2.07 (each 1H, s, NH); ^{19}F NMR ($CDCl_3$) δ=−81.22/27 (3F, s, 3^1-CF_3); MS (APCI) found: m/z 635.4, calcd for $C_{35}H_{38}F_3N_4O_4$: MH^+, 635.3.

*4.2.3. Zinc methyl 3^1-trifluoromethyl-bacteriopheophorbide-d (**1b**)*

Similar to the synthesis of **1a**, zinc-metalation of **6b** (3^1R/S=1:1) gave **1b** as a green solid after FCC (MeOH/CH_2Cl_2=5:95). The 3^1-epimeric mixture (1:1) was separated by HPLC (MeOH/H_2O=8:2, 2.0 ml/min) to afford the first eluted **1b-1** and the second **1b-2** at retention time=64 and 74 min, respectively. Compound **1b-1**: UV–vis (CH_2Cl_2) λ_{max}=654 (rel, 0.82), 606 (0.11), 560 (0.06), 518 (0.03), 424 nm (1.00); ^{1}H NMR ($CDCl_3$/1%C_5D_5N) δ=10.32, 9.57, 8.42 (each 1H, s, 5-, 10-, 20-H), 6.01 (1H, s, 3-OH), 5.20, 5.08 (each 1H, d, J=19 Hz, 13^1-CH_2), 4.39 (1H, dq, J=2, 8 Hz, 18-H), 4.20 (1H, dt, J=8, 2 Hz, 17-H), 3.74 (2H, q, J=8 Hz, 8-CH_2), 3.69, 3.57, 3.49, 3.24 (each 3H, s, 2-, 7-, 12-CH_3, $COOCH_3$), 2.63 (3H, s, 3^1-CH_3), 2.58–2.53, 2.40–2.34, 2.29–2.23, 1.96–1.91 (each 1H, m, 17-CH_2CH_2), 1.70 (3H, d, J=8 Hz, 18-CH_3), 1.69 (3H, t, J=8 Hz, 8^1-CH_3); ^{19}F NMR ($CDCl_3$/1%C_5D_5N) δ=−80.93 (3F, s, 3^1-CF_3); MS (APCI) found: m/z 697.3, calcd for $C_{35}H_{36}F_3N_4O_4Zn$: MH^+, 697.2. Compound **1b-2**: UV–vis (CH_2Cl_2) λ_{max}=654 (rel, 0.82), 606 (0.12), 560 (0.06), 518 (0.04), 424 nm (1.00); ^{1}H NMR ($CDCl_3$/1%C_5D_5N) δ=10.34, 9.57, 8.46 (each 1H, s, 5-, 10-, 20-H), 5.86 (1H, s, 3-OH), 5.18, 5.09 (each 1H, d, J=19 Hz, 13^1-CH_2), 4.40 (1H, dq, J=2, 8 Hz, 18-H), 4.20 (1H, dt, J=8, 2 Hz, 17-H), 3.75 (2H, q, J=8 Hz, 8-CH_2), 3.69, 3.57, 3.48, 3.24 (each 3H, s, 2-, 7-, 12-CH_3, $COOCH_3$), 2.62 (3H, s, 3^1-CH_3), 2.57–2.51, 2.42–2.36, 2.29–2.23, 1.98–1.93 (each 1H, m, 17-CH_2CH_2), 1.70 (3H, d, J=8 Hz, 18-CH_3), 1.69 (3H, t, J=8 Hz, 8^1-CH_3); ^{19}F NMR ($CDCl_3$/1%C_5D_5N) δ=−80.90 (3F, s, 3^1-CF_3); MS (APCI) found: m/z 697.3, calcd for $C_{35}H_{36}F_3N_4O_4Zn$: MH^+, 697.2.

*4.2.4. Methyl 3^1-demethyl-3^1,3^1-bis(trifluoromethyl)-bacteriopheophorbide-d (**6c**)*

Similar to the synthesis of **6a**, reaction of methyl 3-devinyl-3-trifluoroacetyl-pyropheophorbide-*a* (**8c**, 48 mg, 0.077 mmol) with $TMSCF_3$ (200 mg, 0.81 mmol) and $Bu_4NF\cdot 3H_2O$ (5 mg, 0.016 mmol) in THF (5 ml) gave **6c** (15 mg, 29%) as a black solid after FCC (Et_2O/CH_2Cl_2=4:96). UV–vis (CH_2Cl_2) λ_{max}=673 (rel, 0.64), 614 (0.08), 561 (0.07), 510 (0.12), 411 (1.00), 379 nm (0.66); ^{1}H NMR ($CDCl_3$, major/minor=2:1) δ=10.64/9.83 (1H, s, 5-H), 9.43/61 (1H, s, 10-H), 8.75/82 (1H, s, 20-H), 4.98/5.29, 4.94/5.15 (each 1H, d, J=19 Hz, 13^1-CH_2), 5.28/4.40 (1H, s, 3^1-OH), 4.50/55 (1H, q, J=7 Hz, 18-H), 4.19/33 (1H, d, J=9 Hz, 17-H), 3.73/74 (2H, q, J=8 Hz, 8-CH_2), 3.65/60 (3H, s, $COOCH_3$), 3.56/74 (3H, s, 2-CH_3), 3.54/69 (3H, s, 12-CH_3), 3.30/27 (3H, s, 7-CH_3), 2.60–2.52+2.32–2.25+2.19–2.12/2.73–2.67+2.60–2.52+2.32–2.25 (2H+1H+1H/1H+1H+2H, m, 17-CH_2CH_2), 1.74/81 (3H, d, J=8 Hz, 18-CH_3), 1.71/72 (3H, t, J=8 Hz, 8-CH_3), −0.52/0.02, −2.21/−1.99 (each 1H, s, NH); ^{19}F NMR ($CDCl_3$, major/minor=3:2) δ=−73.94/88, −74.82/25 (each 3F, q, J_{FF}=8 Hz, 3^1-CF_3); MS (APCI) found: m/z 689.4, calcd for $C_{35}H_{35}F_6N_4O_4$: MH^+, 689.3.

*4.2.5. Zinc methyl 3^1-demethyl-3^1,3^1-bis(trifluoromethyl)-bacteriopheophorbide-d (**1c**)*

Similar to the synthesis of **1a**, zinc-metalation of **6c** gave **1c** as a green solid after FCC (MeOH/CH_2Cl_2=3:97) and recrystallization from CH_2Cl_2/hexane. UV–vis (CH_2Cl_2) λ_{max}=659 (rel, 0.83), 610 (0.13), 563 (0.08), 523 (0.05), 425 nm (1.00); ^{1}H NMR ($CDCl_3$/1%C_5D_5N, major/minor=3:1) δ=10.83/11.0, 9.59/74, 8.50/48 (each 1H, s, 5-, 10-, 20-H), 5.20, 5.10 (each 1H, d, J=19 Hz, 13^1-CH_2), 4.42 (1H, q, J=7 Hz, 18-H), 4.22 (1H, d, J=8 Hz, 17-H), 3.75 (2H, q, J=8 Hz, 8-CH_2), 3.70, 3.57, 3.45, 3.23/25 (each 3H, s, 2-, 7-, 12-CH_3, $COOCH_3$), 2.59–2.53, 2.42–2.37, 2.28–2.22, 1.98–1.93 (each 1H, m, 17-CH_2CH_2), 1.70 (3H, d, J=8 Hz, 18-CH_3), 1.68 (3H, t, J=8 Hz, 8^1-CH_3); ^{19}F NMR ($CDCl_3$/1%C_5D_5N, major/minor=3:1) δ=−73.76/−72.80, −74.03/−73.31 (each 3F, q, J_{FF}=8 Hz, 3^1-CF_3); MS (APCI) found: m/z 751.3, calcd for $C_{35}H_{33}F_6N_4O_4Zn$: MH^+, 751.2.

4.3. Synthesis of (zinc) methyl 3^1-allyl-bacteriopheophorbides-*d*

*4.3.1. Methyl 3^2-vinyl-bacteriopheophorbide-d (**7a**)*

To an aqueous THF solution (30 ml, THF/H_2O=2:1) of methyl pyropheophorbide-*d* (**8a**, 50 mg, 0.091 mmol), allyl bromide (300 mg, 2.5 mmol), and indium powder (100 mg, 0.87 mmol) were added with stirring. After stirring for 2 h at room temperature under nitrogen atmosphere, indium powder was filtered and the filtrate was extracted with CH_2Cl_2. The organic layer was washed with water three times and dried over Na_2SO_4. The solvents were evaporated and the residue was purified by FCC (Et_2O/CH_2Cl_2=5:95) and then recrystallized from CH_2Cl_2/hexane to give a 1:1 mixture of 3^1R- and 3^1S-**7a** (80%) as a black solid; mp 97–99 °C. See the spectroscopic data of **7a** in Ref. 57.

*4.3.2. Zinc methyl 3^2-vinyl-bacteriopheophorbide-d (**2a**)*

Similar to the synthesis of **1a**, zinc-metalation of **7a** gave **2a** as a 3^1-epimeric mixture (1:1). UV–vis (CH_2Cl_2) λ_{max}=651 (rel, 0.90), 605 (0.18), 426 (1.00), 409 nm (0.81); ^{1}H NMR ($CDCl_3$) δ=9.67/66, 9.46/45, 8.51/50 (each 1H, s, 5-, 10-, 20-H), 6.20/18 (1H, dt, J=1, 8 Hz, 3-CH), 6.04 (1H, ddt, J=17, 10, 7 Hz, 3^2-CH), 5.26/25 (1H, dd, J=17, 2 Hz, 3^3-CH-*trans* to 3^2-CH), 5.15–5.13 (1H, m, 3^3-CH-*cis* to 3^2-CH), 5.17/16, 5.06/05 (each 1H, d, J=20 Hz, 13^1-CH_2), 4.44/43 (1H, q, J=8 Hz, 18-H), 4.24–4.20 (1H, m, 17-H), 3.65 (2H, q, J=8 Hz, 8-CH_2), 3.63/62, 3.60, 3.39/38, 3.23/22 (each 3H, s, 2-, 7-, 12-CH_3, $COOCH_3$), 3.34–3.27, 3.18–3.13 (each 1H, m, 3^1-CH_2), 2.89/85 (1H, br s, OH), 2.68–2.51, 2.30–2.17 (each 2H, m, 17-CH_2CH_2), 1.70 (3H, d, J=8 Hz, 18-CH_3), 1.71/70 (3H, t, J=8 Hz, 8^1-CH_3); MS (FAB) found: m/z 654, calcd for $C_{36}H_{38}N_4O_4Zn$: M^+, 654.

The 3^1-epimeric mixture was separated by HPLC (MeOH/H_2O=9:1, 1.0 ml/min) to afford the first eluted **2a-1** and the second **2a-2** at retention time=51 and 54 min, respectively. Based on Mosher's method reported previously,[42] the stereochemistry of separated **2a-1** and **2a-2** was determined to be 3^1R- and 3^1S-epimers.

*4.3.3. Methyl 3^2-methyl-3^2-vinyl-bacteriopheophorbide-d (**7b**)*

Similar to the synthesis of **7a**, reaction of **8a** with crotyl bromide (1-bromo-2-butene) in dry DMF (30 ml) with additional NaI (100 mg, 0.67 mmol) or in aqueous THF gave a 3^1/3^2-epimeric mixture of **7b** (74 or 64%, respectively) as a black solid; mp 114–116 °C. UV–vis (CH_2Cl_2) λ_{max}=661 (rel, 0.45), 605 (0.07), 537 (0.09), 504 (0.10), 410 nm (1.00); ^{1}H NMR ($CDCl_3$) δ=9.71/70/68/67, 9.51/50/49/49, 8.54/53/51/50 (each 1H, s, 5-, 10-, 20-H), 6.24/6.24/5.87/5.86 (1H, ddd, J=17, 10, 7 Hz, 3^2-CH), 6.01/5.84 (1H, d, J=8 Hz, 3-CH), 5.60/57/03/02 (1H, d, J=17 Hz, 3^3-CH-*trans* to 3^2-CH), 5.47/4.89 (1H, d, J=10 Hz, 3^3-CH-*cis* to 3^2-CH), 5.26/25/25/23, 5.12/11/10/09 (each 1H, d, J=20 Hz, 13^1-CH_2), 4.48/47 (1H, q, J=8 Hz, 18-H), 4.28–4.27 (1H, m, 17-H), 3.71/70 (2H, q, J=8 Hz, 8-CH_2), 3.67/3.66, 3.62, 3.43/43/42/39, 3.26/25 (each 3H, s, 2-, 7-, 12-CH_3, $COOCH_3$), 3.50–3.40 (1H, m, 3^1-CH), 2.98/75 (1H, br s, OH), 2.70–2.52, 2.31–2.25 (each 2H, m, 17-CH_2CH_2), 1.80/79 (3H, d, J=8 Hz, 18-CH_3), 1.67 (3H, t, J=8 Hz, 8^1-CH_3), 1.53/1.52/0.97/0.97 (3H, d, J=8 Hz, 3^2-CH_3), 0.37, −1.76/77/79/80 (each 1H, s, NH); MS (FAB) found: m/z 606, calcd for $C_{37}H_{42}N_4O_4$: M^+, 606.

*4.3.4. Zinc methyl 3^2-methyl-3^2-vinyl-bacteriopheophorbide-d (**2b**)*

Similar to the synthesis of **1a**, zinc-metalation of **7b** gave **2b** as a mixture of 3^1R,3^2R-, 3^1R,3^2S-, 3^1S,3^2R-, and 3^1S,3^2S-forms. UV–vis (CH_2Cl_2) λ_{max}=651 (rel, 0.90), 605 (0.18), 426 (1.00), 409 nm (0.81); ^{1}H NMR ($CDCl_3$) δ=9.55/54, 9.52/52/50/49, 8.31/30/28/28 (each 1H, s, 5-, 10-, 20-H), 6.26/6.25/5.86/5.86 (1H, ddd, J=17, 10, 7 Hz, 3^2-CH), 5.92/92/77/74 (1H, d, J=8 Hz, 3-CH), 5.57/5.55/4.95/4.92 (1H, d, J=17 Hz, 3^3-CH-*trans* to 3^2-CH), 5.44/5.43/4.78/4.77 (1H, d, J=10 Hz, 3^3-CH-*cis* to 3^2-CH), 5.17, 5.06 (each 1H, d, J=20 Hz, 13^1-CH_2), 4.37

(1H, q, J=8 Hz, 18-H), 4.19–4.17 (1H, m, 17-H), 3.74 (2H, q, J=8 Hz, 8-CH_2), 3.69, 3.57, 3.35/33/31/31, 3.24/23 (each 3H, s, 2-, 7-, 12-CH_3, $COOCH_3$), 3.49–3.44 (1H, m, 3^1-CH), 2.57–2.51, 2.39–2.31, 2.28–2.22, 1.96–1.87 (each 1H, m, 17-CH_2CH_2), 1.71 (3H, d, J=8 Hz, 18-CH_3), 1.70 (3H, t, J=8 Hz, 8^1-CH_3), 1.54/1.54/0.93/0.92 (3H, d, J=8 Hz, 3^2-CH_3); MS (FAB) found: m/z 668, calcd for $C_{37}H_{40}N_4O_4Zn$: M^+, 668.

The 3^1/3^2-epimeric mixture was separated by HPLC (MeOH/H_2O=9:1, 1.0 ml/min) to afford **2b-1**, **2b-2**, **2b-3**, and **2b-4** at retention time=41.2, 43.2, 44.9, and 49.2 min, respectively.

*4.3.5. Methyl 3^2,3^2-dimethyl-3^2-vinyl-bacteriopheophorbide-d (**7c**)*

Similar to the synthesis of **7b**, reaction of **8a** with prenyl bromide (1-bromo-3-methyl-2-butene) in DMF/NaI or aqueous THF gave a 1:1 mixture of 3^1R- and 3^1S-**7c** (61 or 42%, respectively) as a black solid; mp 135–137 °C. UV–vis (CH_2Cl_2) λ_{max}=661 (rel, 0.45), 605 (0.07), 537 (0.09), 504 (0.10), 410 nm (1.00); ^{1}H NMR ($CDCl_3$) δ=10.3, 9.54, 8.54 (each 1H, s, 5-, 10-, 20-H), 6.30/29 (1H, dd, J=17, 10 Hz, 3^2-CH), 5.91 (1H, br, 3-CH), 5.35–5.29 (2H, m, 3^3-CH_2), 5.28/27, 5.12 (each 1H, d, J=20 Hz, 13^1-CH_2), 4.49/48 (1H, q, J=7.5 Hz, 18-H), 4.31–4.29 (1H, m, 17-H), 3.70 (2H, q, J=7.5 Hz, 8-CH_2), 3.69, 3.62, 3.35, 3.25 (each 3H, s, 2-, 7-, 12-CH_3, $COOCH_3$), 2.88 (1H, br s, OH), 2.73–2.53, 2.42–2.32 (each 2H, m, 17-CH_2CH_2), 1.80 (3H, d, J=8 Hz, 18-CH_3), 1.71 (3H, t, J=8 Hz, 8^1-CH_3), 1.41/38 (6H, s, 3^2-CH_3), 0.35, −1.00 (each 1H, s, NH); MS (FAB) found: m/z 620, calcd for $C_{38}H_{44}N_4O_4$: M^+, 620.

*4.3.6. Zinc methyl 3^2,3^2-dimethyl-3^2-vinyl-bacteriopheophorbide-d (**2c**)*

Similar to the synthesis of **1a**, zinc-metalation of **7c** gave **2c** as a 3^1-epimeric mixture (1:1). UV–vis (CH_2Cl_2) λ_{max}=651 (rel, 0.90), 605 (0.18), 426 (1.00), 409 nm (0.81); ^{1}H NMR ($CDCl_3$) δ=9.94, 9.54, 8.30 (each 1H, br s, 5-, 10-, 20-H), 6.04 (1H, dd, J=17, 10 Hz, 3^2-CH), 5.80 (1H, br s, 3-CH), 5.32–5.25 (2H, m, 3^3-CH_2), 5.18/17, 5.06 (each 1H, d, J=20 Hz, 13^1-CH_2), 4.36 (1H, q, J=8 Hz, 18-H), 4.19–4.17 (1H, m, 17-H), 3.74 (2H, q, J=8 Hz, 8-CH_2), 3.68, 3.57/56, 3.49, 3.23 (each 3H, s, 2-, 7-, 12-CH_3, $COOCH_3$), 2.57–2.51, 2.38–2.22 (each 2H, m, 17-CH_2CH_2), 1.94–1.92 (6H, m, 3^2-CH_3), 1.94–1.92 (3H, m, 18-CH_3), 1.71 (3H, t, J=8 Hz, 8^1-CH_3); MS (FAB) found: m/z 682, calcd for $C_{38}H_{42}N_4O_4Zn$: M^+, 682.

The 3^1-epimeric mixture was separated by HPLC (MeOH/H_2O=9:1, 1.0 ml/min) to afford the first eluted **2c-1** and the second **2c-2** at retention time=56 and 59 min, respectively.

4.4. Synthesis of methyl 3^1-alkyl-bacteriopheophorbides-*d*

*4.4.1. Methyl 3^2-methyl-bacteriopheophorbide-d (**9b**)*

According to reported procedures,[42] Grignard reaction of **8a** with ethyl magnesium iodide gave **9b** as a 3^1-epimeric mixture (1:1) in 75% yield based on consumed **8a**: black solid. UV–vis (CH_2Cl_2) λ_{max}=661 (rel, 0.47), 605 (0.08), 536 (0.10), 505 (0.10), 410 nm (1.00); ^{1}H NMR ($CDCl_3$) δ=9.71, 9.53, 8.53 (each 1H, s, 5-, 10-, 20-H), 6.16/6.15 (1H, t, J=7 Hz, 3-CH), 5.27, 5.12 (each 1H, d, J=20 Hz, 13^1-CH_2), 4.49/4.48 (1H, dq, J=2, 7 Hz, 18-H), 4.31/4.30 (1H, dt, J=8, 2 Hz, 17-H), 3.71 (2H, q, J=8 Hz, 8-CH_2), 3.68, 3.61, 3.42, 3.26 (each 3H, s, 2-, 7-, 12-CH_3, $COOCH_3$), 2.78–2.61, 2.61–2.44, 2.40–2.22 (each 2H, m, 3^1-, 17-, 17^1-CH_2), 1.81/1.80 (3H, d, J=7 Hz, 18-CH_3), 1.70 (3H, t, J=8 Hz, 8^1-CH_3), 1.14 (3H, t, J=7 Hz, 3^2-CH_3), 0.08, −1.94 (each 1H, s, NH); MS (FAB) found: m/z 580, calcd for $C_{35}H_{40}N_4O_4$: M^+, 580.

*4.4.2. Methyl 3^2,3^2-dimethyl-bacteriopheophorbide-d (**9c**)*

According to reported procedures,[42] Grignard reaction of **8a** with isopropyl magnesium chloride gave **9b** as a 3^1-epimeric mixture: black solid. UV–vis (CH_2Cl_2) λ_{max}=661 (rel, 0.49), 605 (0.11), 536 (0.12), 505 (0.12), 410 nm (1.00); ^{1}H NMR ($CDCl_3$) δ=9.68, 9.49, 8.52/8.51 (each 1H, s, 5-, 10-, 20-H), 5.79 (1H, d, J=9 Hz, 3-CH), 5.25/5.24, 5.09/5.08 (each 1H, d, J=20 Hz, 13^1-CH_2), 4.49 (1H, dq, J=2, 7 Hz, 18-H), 4.31 (1H, dt, J=8, 2 Hz, 17-H), 3.69 (2H, q, J=8 Hz, 8-CH_2), 3.65, 3.61, 3.42, 3.26, (each 3H, s, 2-, 7-, 12-CH_3, $COOCH_3$), 2.90–2.94 (1H, m, 3^1-CH), 2.71–2.51, 2.36–2.22 (each 2H, m, 17-CH_2CH_2), 1.80/1.79 (3H, d, J=7 Hz, 18-CH_3), 1.69 (3H, t, J=8 Hz, 8^1-CH_3), 1.51, 0.91 (each 3H, d, J=7 Hz 3^2-$(CH_3)_2$), 0.08, −1.94 (each 1H, s, NH); MS (FAB) found: m/z 594, calcd for $C_{36}H_{42}N_4O_4$: M^+, 594.

Acknowledgements

We thank Mrs. Yoshiyuki Shimono and Takuya Hibino, and Dr. Michio Kunieda of Ritsumeikan University for their assistance in the experiments. This work was partially supported by Grant-in-Aid for Scientific Research (B) (No. 19350088) from the Japan Society for the Promotion of Science (JSPS).

Supplementary data

Supplementary data associated with this article can be found in the online version, at doi:10.1016/j.tet.2008.11.015.

References and notes

1. Katz, J. J.; Bowman, M. K.; Michalski, T. J.; Worcester, D. L. In *Chlorophylls*; Scheer, H., Ed.; CRC: Boca Raton, FL, 2001; pp 211–235; Section 1.8.
2. Blankenship, R. E.; Olson, J. M.; Miller, M. In *Anoxygenic Photosynthetic Bacteria*; Blankenship, R. E., Madigan, M. T., Bauer, C. E., Eds.; Kluwer Academic: Dordrecht, The Netherlands, 1995; Chapter 20, pp 399–435.
3. Olson, J. M. *Photochem. Photobiol.* **1998**, *67*, 61.
4. Frigaard, N.-U.; Chew, A. G. M.; Li, H.; Maresca, J. A.; Bryant, D. A. *Photosynth. Res.* **2003**, *78*, 93.
5. Balaban, T. S. *Acc. Chem. Res.* **2005**, *38*, 612.
6. Saga, Y.; Shibata, Y.; Itoh, S.; Tamiaki, H. *J. Phys. Chem. B* **2007**, *111*, 12605.
7. Linnanto, J. M.; Korppi-Tommola, J. E. I. *Photosynth. Res.* **2008**, *96*, 227.
8. Arellano, J. B.; Torkkeli, M.; Tuma, R.; Laurinmäki, P.; Melø, T. B.; Ikonen, T. P.; Butcher, S. J.; Serimaa, R. E.; Pšenčík, J. *Langmuir* **2008**, *24*, 2035.
9. Sridharan, A.; Muthuswamy, J.; LaBelle, J. T.; Pizziconi, V. B. *Langmuir* **2008**, *24*, 8078.
10. Tamiaki, H.; Miyatake, T.; Tanikaga, R.; Holzwarth, A. R.; Schaffner, K. *Angew. Chem., Int. Ed.* **1996**, *35*, 772.
11. Prokhorenko, V. I.; Holzwarth, A. R.; Müller, M. G.; Schaffner, K.; Miyatake, T.; Tamiaki, H. *J. Phys. Chem. B* **2002**, *106*, 5761.
12. de Boer, I.; Matysik, J.; Erkelens, K.; Sasaki, S.; Miyatake, T.; Yagai, S.; Tamiaki, H.; Holzwarth, A. R.; de Groot, H. J. M. *J. Phys. Chem. B* **2004**, *108*, 16556.
13. Balaban, T. S.; Tamiaki, H.; Holzwarth, A. R. *Top. Curr. Chem.* **2005**, *258*, 1.
14. Tamiaki, H. *Photochem. Photobiol. Sci.* **2005**, *4*, 675.
15. Zietz, B.; Prokhorenko, V. I.; Holzwarth, A. R.; Gillbro, T. *J. Phys. Chem. B* **2006**, *110*, 1388.
16. Katterle, M.; Prokhorenko, V. I.; Holzwarth, A. R.; Jesorka, A. *Chem. Phys. Lett.* **2007**, *447*, 284.
17. Kakitani, Y.; Harada, K.; Mizoguchi, T.; Koyama, Y. *Biochemistry* **2007**, *46*, 6513.
18. Ptaszek, M.; Yao, Z.; Savithri, D.; Boyle, P. D.; Lindsey, J. S. *Tetrahedron* **2007**, *63*, 12629.
19. Mizoguchi, T.; Tamiaki, H. *Bull. Chem. Soc. Jpn.* **2007**, *80*, 2196.
20. Shibata, R.; Koike, K.; Hori, H.; Tamiaki, H. *Chem. Lett.* **2008**, *37*, 532.
21. Tamiaki, H.; Michitsuji, T.; Shibata, R. *Photochem. Photobiol. Sci.* **2008**, *7*, 1225.
22. Alster, J.; Zupcanova, A.; Vacha, F.; Pšenčík, J. *Photosynth. Res.* **2008**, *95*, 183.
23. Huijser, A.; Suijkerbuijk, B. M. J. M.; Gebbink, R. J. M. K.; Savenije, T. J. S.; Siebbeles, L. D. A. *J. Am. Chem. Soc.* **2008**, *130*, 2485.
24. Röger, C.; Miloslavina, Y.; Brunner, D.; Holzwarth, A. R.; Würthenr, F. *J. Am. Chem. Soc.* **2008**, *130*, 5929.
25. Huber, V.; Sengupta, S.; Würthner, F. *Chem.—Eur. J.* **2008**, *14*, 7791.
26. Zupcanova, A.; Arellano, J. B.; Bina, D.; Kopecky, J.; Pšenčík, J.; Vacha, F. *Photochem. Photobiol.* **2008**, *84*, 1187.
27. Jochum, T.; Reddy, C. M.; Eichhöfer, A.; Buth, G.; Szmytkowski, J.; Kalt, H.; Moss, D.; Balaban, T. S. *Proc. Natl. Acad. Sci. U.S.A.* **2008**, *105*, 12736.
28. Tamiaki, H.; Amakawa, M.; Shimono, Y.; Tanikaga, R.; Holzwarth, A. R.; Schaffner, K. *Photochem. Photobiol.* **1996**, *63*, 92.
29. Tamiaki, H. *Coord. Chem. Rev.* **1996**, *148*, 183.
30. Jesorka, A.; Balaban, T. S.; Holzwarth, A. R.; Schaffner, K. *Angew. Chem., Int. Ed.* **1996**, *35*, 2861.
31. Yagai, S.; Miyatake, T.; Tamiaki, H. *J. Org. Chem.* **2002**, *67*, 49.
32. Kunieda, M.; Tamiaki, H. *Eur. J. Org. Chem.* **2006**, 2352.
33. Kunieda, M.; Tamiaki, H. *J. Org. Chem.* **2007**, *72*, 2443.
34. Tamiaki, H.; Shibata, R.; Mizoguchi, T. *Photochem. Photobiol.* **2007**, *83*, 152.
35. Tamiaki, H.; Yoshimura, H.; Shimamura, Y.; Kunieda, M. *Photosynth. Res.* **2008**, *95*, 223.
36. Kunieda, M.; Tamiaki, H. *J. Org. Chem.* **2008**, *73*, 7686.

37. Tamiaki, H.; Takeuchi, S.; Tanikaga, R.; Balaban, S. T.; Holzwarth, A. R.; Schaffner, K. *Chem. Lett.* **1994**, 401.
38. Balaban, T. S.; Tamiaki, H.; Holzwarth, A. R.; Schaffner, K. *J. Phys. Chem. B* **1997**, *101*, 3424.
39. Tamiaki, H.; Takeuchi, S.; Tsudzuki, S.; Miyatake, T.; Tanikaga, R. *Tetrahedron* **1998**, *54*, 6699.
40. Tamiaki, H.; Holzwarth, A. R.; Schaffner, K. *J. Photochem. Photobiol., B* **1992**, *15*, 355.
41. Yagai, S.; Miyatake, T.; Shimono, Y.; Tamiaki, H. *Photochem. Photobiol.* **2001**, *73*, 153.
42. Tamiaki, H.; Kitamoto, H.; Nishikawa, A.; Hibino, T.; Shibata, R. *Bioorg. Med. Chem.* **2004**, *12*, 1657.
43. Sasaki, S.; Kotegawa, Y.; Tamiaki, H. *Tetrahedron Lett.* **2006**, *47*, 4849.
44. Tamiaki, H.; Hamada, K.; Kunieda, M. *Tetrahedron* **2008**, *64*, 5721.
45. Miyatake, T.; Tamiaki, H. *J. Photochem. Photobiol., C* **2005**, *6*, 89.
46. Sasaki, S.; Mizoguchi, T.; Tamiaki, H. *Tetrahedron* **2005**, *61*, 8041.
47. O'Hagan, D.; Rzepa, H. S. *Chem. Commun.* **1997**, 645.
48. Mikami, K.; Itoh, Y.; Yamanaka, M. *Chem. Rev.* **2004**, *104*, 1.
49. Jäckel, C.; Salwiczek, M.; Koksch, B. *Angew. Chem., Int. Ed.* **2006**, *45*, 4198.
50. Ahmed, A.; Bragg, R. A.; Clayden, J.; Lai, L. W.; McCarthy, C.; Pink, J. H.; Westlund, N.; Yasin, S. A. *Tetrahedron* **1998**, *54*, 13277.
51. Kureishi, Y.; Tamiaki, H. *J. Porphyrins Phthalocyanines* **1998**, *2*, 159.
52. Rotational barriers of methyl (3^1-substituted) bacteriopheophorbides-*d* **9a** [3-CHMeOH], **6a** [3-CH(CF_3)OH], and **6b** [3-CMe(CF_3)OH] were calculated to be 9, 10, and 11 kcal mol^{-1}, respectively, from molecular modeling. These values were smaller than that of **6c** [3-C(CF_3)$_2$OH] as expected. Molecular modeling calculation also indicated that the right rotamer of **6c** in Figure 6 was 0.5 kcal mol^{-1} more stable than the left. The energy difference led to ca. a 1:2 mixture of **6c** at room temperature, which was consistent with the observed ^{1}H NMR data in $CDCl_3$. The major rotamer of **6c** in a solution at room temperature would be assigned as the right drawing in Figure 6. The same stability was observed in di(*tert*-butyl)-*o*-tolyl-carbinol (lower of Fig. 6).[53]
53. Lomas, J. S.; Luong, P. K.; Dubois, J.-E. *J. Org. Chem.* **1977**, *42*, 3394.
54. Ōki, M. *Angew. Chem., Int. Ed. Engl.* **1976**, *15*, 87.
55. Tamiaki, H.; Shimono, Y.; Rattray, A. G. M.; Tanikaga, R. *Bioorg. Med. Chem. Lett.* **1996**, *6*, 2085.
56. Augé, J.; Lubin-Germain, N.; Uziel, J. *Synthesis* **2007**, 1739.
57. Yagai, S.; Tamiaki, H. *J. Chem. Soc., Perkin Trans. 1* **2001**, 3135.
58. Kwon, J. S.; Pae, A. N.; Choi, K. I.; Koh, H. Y.; Kim, Y.; Cho, Y. S. *Tetrahedron Lett.* **2001**, *42*, 1957.
59. Nair, V.; Jayan, C. N. *Tetrahedron Lett.* **2000**, *41*, 1091.
60. The solubility of **2c-1** in MeOH/H_2O=9:1 was different from that of diastereomeric **2c-2**. Since the concentrated solution was filtered and injected to an HPLC system, the HPLC area of **2c-2** was smaller than that of **2c-1** as shown in Figure 7c.
61. Leroux, F. *ChemBioChem* **2004**, *5*, 644.
62. Tamiaki, H.; Yagai, S.; Miyatake, T. *Bioorg. Med. Chem.* **1998**, *6*, 2171.